Utilization of cross-linked chitosan/bentonite composite in the removal of methyl orange from aqueous solution

Ruihua Huang, Qian Liu, Lujie Zhang and Bingchao Yang

ABSTRACT

A kind of biocomposite was prepared by the intercalation of chitosan in bentonite and the cross-linking reaction of chitosan with glutaraldehyde, which was referred to as cross-linked chitosan/bentonite (CCS/BT) composite. Adsorptive removal of methyl orange (MO) from aqueous solutions was investigated by batch method. The adsorption of MO onto CCS/BT composite was affected by the ratio of chitosan to BT and contact time. pH value had only a minor impact on MO adsorption in a wide pH range. Adsorption kinetics was mainly controlled by the pseudo-second-order kinetic model. The adsorption of MO onto CCS/BT composite followed the Langmuir isotherm model, and the maximum adsorption capacity of CCS/BT composite calculated by the Langmuir model was 224.8 mg/g. Experimental results indicated that this adsorbent had a potential for the removal of MO from aqueous solutions.

Key words | adsorption, chitosan/bentonite composite, isotherm, methyl orange

Ruihua Huang (corresponding author)
Qian Liu
Lujie Zhang
College of Science,
Northwest A&F University,
Yangling,
Shaanxi 712100,
China
E-mail: *hrh20022002@163.com*

Bingchao Yang
Xi'an Institute of Geology and Mineral Resource,
Xi'an,
Shaanxi 710054,
China

INTRODUCTION

Synthetic dyestuffs widely exist in the effluents of industries such as textile, rubber, leather, and plastics. Discharging even a small amount of dyes into water resources can destroy the biotic environment of ecosystems. Therefore, several techniques are applied to remove dyes from wastewater, such as membrane filtration, oxidation, advanced oxidation, coagulation, biological treatment, electrochemical process, and adsorption Among these methods, adsorption can be thought to be the most efficient process for the treatment of wastewater owing to high removal efficiency for different types of effluents, ease of operation, availability of a variety of cheap adsorbents, and the absence of sludge and harmful by-product formation (Hena 2010).

At present, many types of adsorbents like alum sludge (Tripathy *et al*. 2006), chitosan (Bansiwal *et al*. 2009; Pitakpoolsil & Hunsom 2013), clays (Sun *et al*. 2013; Zha *et al*. 2013; Fan *et al*. 2014), biocomposite (Saravanan *et al*. 2013; Nair *et al*. 2014), and agricultural waste (Nguyen *et al*. 2013; Cao *et al*. 2014) have been tried. Among these materials, biocomposite has attracted great attention because of its high adsorption capacity and good mechanical strength. Chitosan, a natural polymer, is an excellent biosorbent for the removal of metal ions and dyes from wastewater due to its non-toxicity, biocompatibility, and biodegradability. Also, chitosan possesses various functional groups in its structure such as amine, hydroxyl, and acetamide groups that can be involved in the adsorption process (Wan Ngah *et al*. 2011). However, chitosan still has some drawbacks such as poor mechanical strength, easy agglomeration, and its solubility in dilute acids. To overcome these problems, the synthesis of biocomposite has presented a novel approach. Recently composites of chitosan such as chitosan–zeolite (Wan Ngah *et al*. 2012, 2013; Nesic *et al*. 2013), chitosan–fly ash (Wen *et al*. 2011), and chitosan–montmorillonite (Nesic *et al*. 2012; Pereira *et al*. 2013) were prepared in various ways in order to remove environmental pollutants from wastewater.

Clay materials are made of hydrous aluminosilicates, which have high cation exchange capacity and large-specific surface areas. Moreover, clay minerals are abundant, chemically and mechanically stable, and low-cost, making it an attractive immobilization material for chitosan (Nesic *et al*. 2012). Among the mineral clays, bentonite has been highlighted for the preparation of chitosan composites because of its high cationic exchange capacity and the possibility of lamellar expansion (Anirudhan *et al*. 2010; Anirudhan & Rijith 2012), which provides greater versatility in the interaction and intercalation of bulky molecules such as natural polymers. Therefore, in

doi: 10.2166/wst.2014.478

this work, a combination of physical and chemical modifications was applied in the preparation of cross-linked chitosan/bentonite (CCS/BT) composite, where chitosan would intercalate in bentonite and be cross-linked with glutaraldehyde (GLA). Methyl orange (MO) was chosen as a model dye in this study, because it is a common water-soluble azo dye, which is widely used in chemical, textile, and paper industries, and it is a serious hazard to the environment. The color index number of MO is 13025. Removal of MO from aqueous solutions was investigated by batch method. The factors affecting the adsorption of MO onto CCS/BT composite including the ratio of chitosan to bentonite, initial pH value of MO solution, and contact time were investigated in detail.

MATERIALS AND METHODS

Materials

Chitosan was purchased from Sinopharm Group Chemical Reagent Company Limited (China). Bentonite powder with a particle size of 200 mesh was acquired from the chemical factory of Shentai, Xinyang, Henan, China. MO was supplied by Sigma Chemical Company, and used as adsorbate in this study. MO concentrations were measured using a UV–Vis spectrometer at a wavelength corresponding to the maximum absorbance for MO: 464 nm. All other reagents were of analytical grade. The pH value of MO solutions was adjusted by adding 0.1 M HCl or NaOH solutions.

Preparation of CCS/BT composite

CCS/BT composite was prepared according to the references (Tirtom *et al*. 2012; Pereira *et al*. 2013) with some modifications. Chitosan powder (2 g) was dissolved in 100 mL of 2% (wt/v) acetic acid solution. About 2 g of bentonite was added and then mixed for 2 h at 20 °C. GLA solution (25 wt%) was added into the mixed solution and the ratio of GLA to chitosan was approximately 5 mL/g of chitosan. Cross-linking reaction occurred for 23 h at 60 °C and then the CCS/BT composite was washed using distilled water to remove any free GLA and dried in an oven at 60 °C for 24 h. After drying, this composite was ground and sieved. The composite with 200 mesh particle size was collected and utilized for the batch experiments. The resultant composite was referred to as CCS/BT composite.

Characterization of CCS/BT composite

X-ray diffraction (XRD) patterns were obtained for natural bentonite and CCS/BT composite using a Shimadzu XD3A diffractometer equipped with a monochromatic Cu Ka source operating at 40 kV and 30 mA. The diffraction patterns were recorded from 3 ° to 55 ° with a scan rate of 0.02 °/s.

Adsorption of MO onto CCS/BT composite

Batch experiments were performed in a set of 250 mL flasks that contained 50 mL MO solutions of different initial concentrations and 0.03 g adsorbent. The flasks were then agitated at 200 rpm on a thermostated shaker. After a defined time, the supernatant was filtered through filter paper to determine the residual concentrations. The adsorbate concentrations in the initial and residual aqueous solutions were measured to calculate the removal efficiency and adsorption capacity. To study the effect of the ratio of chitosan to bentonite on MO adsorption, adsorption experiments were conducted at 293 K by using 50 mL of solution with MO concentration of 100 mg/L and 0.03 g of adsorbent dosage. To study the effect of initial pH value on MO adsorption by CCS/BT composite, adsorption experiments were performed at 293 K by using 50 mL of solution with MO concentrations of 50 and 100 mg/L and 0.03 g of adsorbent dosage. Effect of contact time was studied at 293 K, with initial MO concentrations of 100, 150, 200, and 400 mg/L, by varying contact time from 5 to 120 min. All experimental data were the average of triplicate determinations and the relative errors were about 5%.

Adsorption kinetics

Experimental data generated from MO adsorption tests using CCS/BT composite were evaluated by pseudo-first- and second-order kinetic, Elovich kinetic and intraparticle diffusion models to understand the dynamics of the adsorption process. The pseudo-first-order kinetic model, also known as the Lagergren kinetic equation as expressed in Equation (1), is widely employed to understand the kinetic behavior of the adsorption reactions (Ho 2004)

$$\frac{1}{q_t} = \frac{k_1}{q_e t} + \frac{1}{q_e} \tag{1}$$

where q_e and q_t are the amounts of adsorbate adsorbed (mg/g) at equilibrium and at contact time t (min),

respectively, and k_1 is the rate constant of the pseudo-first-order adsorption (min^{-1}).

The pseudo-second-order kinetic model is given by Equation (2) (Repo *et al.* 2013)

$$\frac{t}{q_t} = \frac{1}{k_2 q_e^2} + \frac{1}{q_e} t \tag{2}$$

where k_2 is the rate constant of the pseudo-second-order adsorption (g/(mg min)).

In reactions involving chemisorption of adsorbates on solid surface, with no desorption products, the sorption process may be described by the Elovich equation, given by Equation (3) (Kellner *et al.* 1998)

$$q_t = \frac{1}{\beta}\ln(\alpha\beta) + \frac{1}{\beta}\ln(t) \tag{3}$$

where α is the initial adsorption rate (mg/(g min)) and β is related to the extent of surface coverage and activation energy for chemisorption (g/mg).

The pseudo-first-order and pseudo-second-order kinetic models cannot identify the diffusion mechanism, so kinetic results need to be analyzed by the intraparticle diffusion model. The intraparticle diffusion was explored by using Equation (4) (Weber & Morris 1964)

$$q_t = k_p t^{0.5} + B \tag{4}$$

where k_p is the rate constant of the intraparticle diffusion (mg/(g $min^{0.5}$)) and B is a constant that gives an idea about the thickness of the boundary layer, i.e., the larger the value of B, the greater is the boundary layer effect.

Isothermal study

Adsorption isotherms were used to evaluate the equilibrium data. Langmuir and Freundlich models were often used to analyze the data in solid–liquid adsorption systems. The Langmuir adsorption isotherm is based on the assumption that the adsorbate molecules form a monolayer on the surface of the adsorbent. Adjacent adsorbed molecules do not interact; i.e., the adsorption of adsorbate at a particular site is independent whether or not the neighboring sites are adsorbed. The Langmuir isotherm can be represented as Equation (5) (Harmoudi *et al.* 2014)

$$\frac{C_e}{q_e} = \frac{1}{Qb} + \frac{C_e}{Q} \tag{5}$$

where C_e is the MO concentration at equilibrium (mg/L), q_e is the amount of MO adsorbed per unit of adsorbent at equilibrium (mg/g), Q is the maximum amount of adsorption with complete monolayer coverage on the adsorbent surface (mg/g), and b is the Langmuir constant, which is related to the energy of adsorption (L/mg). The Langmuir constant can be estimated from the linear plot of C_e/q_e versus C_e.

The Freundlich isotherm is applicable for heterogeneous adsorption reactions and involves the formation of a multilayer. The Freundlich isotherm can be represented as Equation (6) (Li *et al.* 2012):

$$\log q_e = \log K_f + \frac{1}{n}\log C_e \tag{6}$$

where K_f ((mg/g) $(L/mg)^{1/n}$) and n are Freundlich constants related to adsorption capacity and heterogeneity factor, respectively. The values of K_f and n can be obtained from the slope and intercept of the plot of $\log q_e$ versus $\log C_e$.

RESULTS AND DISCUSSION

Characterization of CCS/BT composite

Figure 1 shows the XRD patterns of natural bentonite and CCS/BT composite. XRD analysis can tell whether chitosan entered into the interlayer spacing of bentonite. The XRD pattern for bentonite exhibited a typical reflection of montmorillonite at $2\theta = 6.56^\circ$. After bentonite interacted with chitosan, this peak shifted to a lower diffraction angle, suggesting chitosan intercalated in bentonite. Also, a decrease in the intensity of this peak was observed. This

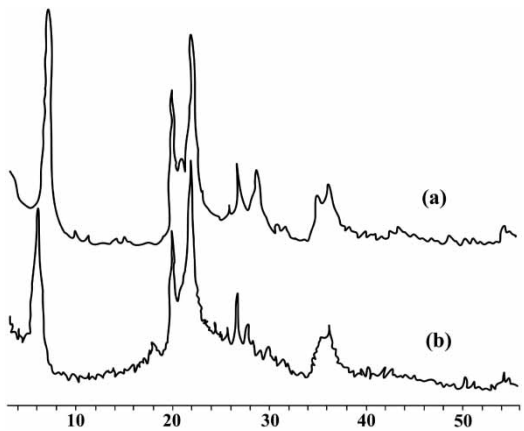

Figure 1 | XRD patterns of natural bentonite (a) and cross-linked chitosan/bentonite composite (b).

decrease may be attributed to a slight distortion of the intrinsic lattice arrangement of the silicate layers, and a decrease in the crystallinity caused by the interaction of bentonite with chitosan. These results indicated the incorporation of chitosan into the interlayer spacing of bentonite. A similar result was also observed by Pereira *et al.* (2013) for the intercalation of chitosan into the interlayer spacing of KSF-Na montmorillonite. This increase in interlayer spacing would facilitate the adsorption of adsorbate onto adsorbent.

Effect of the ratio of chitosan to bentonite on MO adsorption

Figure 2 shows the effect of the ratio of chitosan to bentonite in CCS/BT composite on MO adsorption. The composite allowed higher removal efficiencies toward MO as compared with both cross-linked chitosan and bentonite. The maximum removal efficiency was observed at the ratio of 2/2. This dramatically high removal efficiency may be due to the big interlayer spacing resulting from the intercalation of chitosan in bentonite and the strong interaction between this composite and dye molecules. However, the removal efficiency toward MO reduced with a decrease in this ratio, suggesting that increasing content of bentonite in CCS/BT composite was adverse to the adsorption of MO onto CCS/BT composite. Therefore, the ratio of chitosan to bentonite in CCS/BT composite was controlled at 2/2 in this study.

Effect of pH value of MO solution

The initial pH value of dye solution is recognized as an important operational parameter which can significantly affect the adsorption mechanism between the dye molecules and the adsorbent. The effect of pH value of MO solutions on MO adsorption is shown in Figure 3. The results revealed that the changes of pH values appeared to have little impact on MO adsorption using CCS/BT composite. Over 95 and 92% removal efficiencies for MO solutions with 50 and 100 mg/L were obtained at pH 3–11. Only a slight decrease in MO adsorption was observed as the pH increased over 10. Two possible mechanisms of MO adsorption on CCS/BT composite may be occurring: (a) electrostatic interactions between amine groups from chitosan and anionic dye and (b) chemical reaction through various reactive groups from MO and adsorbent: i.e., MO can form hydrogen bonds with the OH groups of chitosan owing to the high electronegativity of its O, N, and S atoms. In acidic medium, the NH_2 groups of chitosan were protonated into $-NH_3^+$. The strong electrostatic interaction between positively charged $-NH_3^+$ and anion groups of dye resulted in high removal efficiency. In alkaline solution, the NH_2 groups of chitosan were deprotonated and abundant OH^- ions created a competitive environment with anion groups of MO for the adsorption sites; thus the removal efficiency decreased. Yao *et al.* (2011) also reported a similar result about the MO adsorption onto multi-walled carbon nanotubes. However, more than 90% MO can be removed by

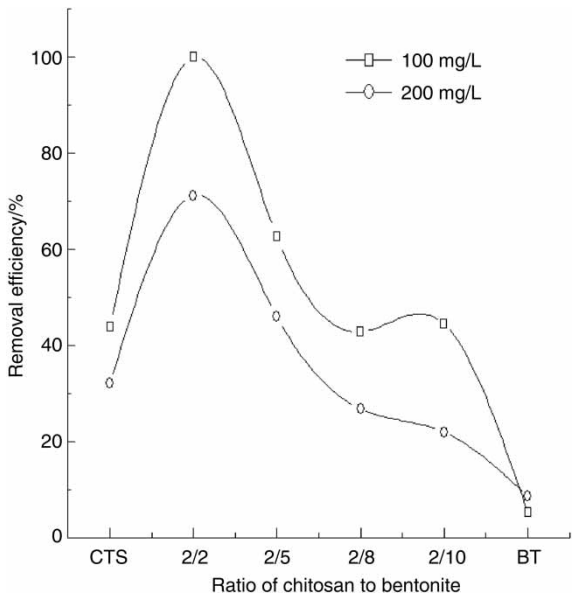

Figure 2 | Effect of ratio of chitosan to bentonite on MO adsorption.

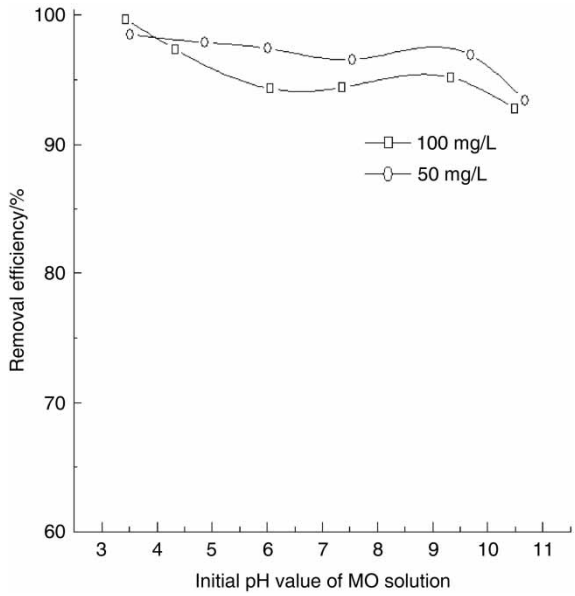

Figure 3 | Effect of initial pH of MO solution on MO adsorption.

CCS/BT composite at natural pH. Therefore, the pH value of MO solutions was unadjusted in later adsorption experiments.

Effect of contact time

Equilibrium time is one of the most important parameters in the design of economical wastewater treatment systems (Chen *et al*. 2010). To investigate the kinetics of adsorption, four different initial concentrations of MO were chosen, 100, 150, 200, and 400 mg/L. Figure 4 shows these plots of adsorption capacity (q_t) of MO onto CCS/BT composite versus contact time for different initial MO concentrations. As seen in Figure 4, q_t value at equilibrium time increased evidently from 156.8 to 219.3 mg/g with the increase in initial concentration from 100 to 400 mg/L. The initial concentration played an important role in the adsorption capacity of MO on CCS/BT composite. An increase in the adsorption capacity of MO with increasing initial MO concentration might be attributed to an increase in the driving force of concentration gradient with the increase in the initial concentration (Wu *et al*. 2001). The adsorption was initially rapid, and then slowed, perhaps because a large number of vacant surface sites were available for adsorption during the initial stage, and then the remaining vacant surface sites were difficult to occupy because of the repulsive forces between the dye molecules on the CCS/BT composite and the bulk phase. For the sake of the attainment of equilibrium, an equilibrium time of 100 min was considered to be optimum in further experiments.

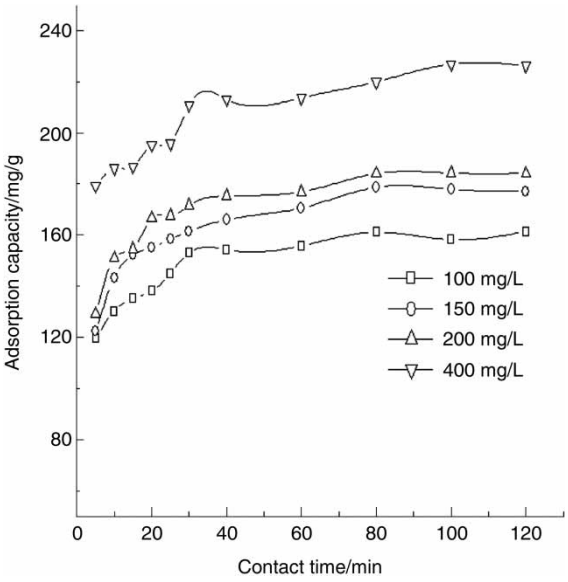

Figure 4 | Effect of contact time on MO adsorption.

Adsorption kinetics

The kinetics of MO adsorption on CCS/BT composite was studied at natural pH and 293 K for several initial concentrations from 100 to 400 mg/L under predetermined time intervals. Kinetic models were applied on the experimental data to investigate the potential rate-determining step of the adsorption process. Table 1 presents the parameters for pseudo-first-order, pseudo-second-order, and Elovich kinetic models of MO adsorption on CCS/BT composite, while in Figure 5 are shown all the investigated kinetic models. Data presented in Table 1 show that the adsorption process of MO on CCS/BT composite followed the pseudo-second-order rather than pseudo-first-order model. The experimentally calculated values of q_e at various concentrations of MO were in a good agreement with theoretical calculated values. Further, the values of correlation coefficients (R^2) for the pseudo-first-order kinetic model were lower than the ones for the pseudo-second-order kinetic model. Also, relatively high values of correlation coefficients for the Elovich equation were observed, indicating that the chemisorption involving valence forces through sharing or exchange of electrons between MO and active sites on the surface of CCS/BT composite occurred. Also, it was not difficult to find that these plots of q_t versus the square root of

Table 1 | Pseudo-first-order, pseudo-second-order and Elovich kinetic models parameters for the adsorption of MO onto cross-linked chitosan/bentonite composite

		Pseudo-first-order model			Pseudo-second-order model			Elovich model		
C_0/mg/L	$q_{e,exp}$/mg/g	R^2	k_1/min^{-1}	$q_{e,cal}$/mg/g	R^2	k_2/g/(mg min)	$q_{e,cal}$/mg/g	R^2	β/g/mg	α/mg/(g min)
100	161.3	0.9455	1.8571	148.7	0.9998	0.0022	163.9	0.9701	0.0674	6404
150	177.9	0.9869	2.3422	167.3	0.9998	0.0017	182.8	0.9767	0.0600	8052
200	184.2	0.9884	2.2481	175.2	0.9999	0.0018	188.7	0.9645	0.0607	14086
400	226.3	0.8526	1.3478	217.4	0.9996	0.0013	231.5	0.9709	0.0608	135578

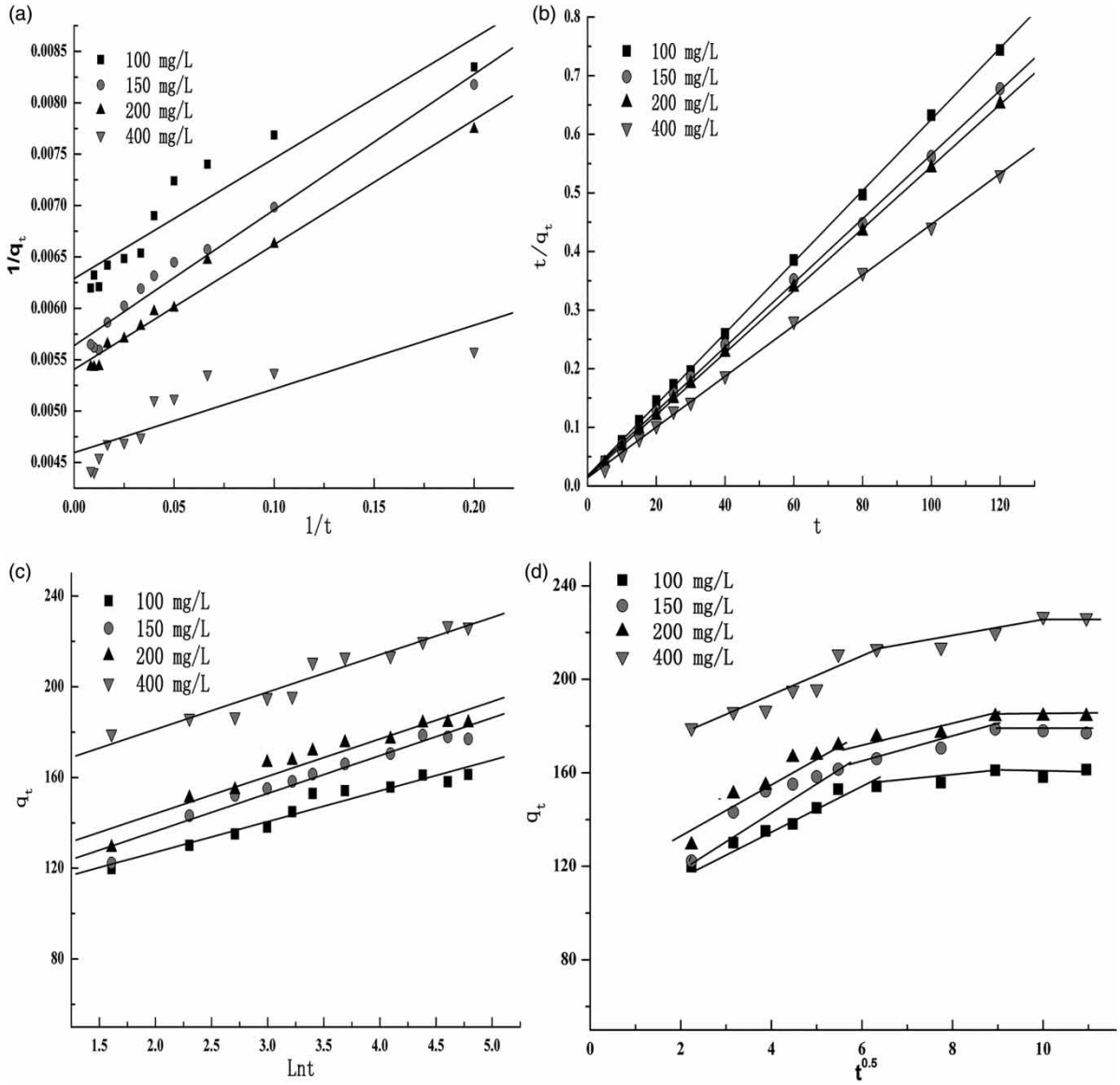

Figure 5 | Adsorption kinetic models of MO by cross-linked chitosan/bentonite composite: (a) pseudo-first-order kinetic model; (b) pseudo-second-order kinetic model; (c) Elovich model; (d) intraparticle diffusion model.

time obtained were not linear over the whole time range, indicating that more than one step was involved in the adsorption of MO. If intraparticle diffusion is the only rate-controlling step, the plot should pass through the origin, otherwise the boundary layer diffusion affects the adsorption to some degree. These plots were not passing through the origin, indicating that intraparticle diffusion was not the only rate-determining factor, and more than one step was involved in the adsorption of MO. Table 2 presents a comparison of intraparticle diffusion rate parameters for the adsorption of MO onto CCS/BT composite. The results indicated $kp_1 > kp_2 > kp_3$. This was not surprising because the concentration of MO left in the solutions gradually decreased with increasing adsorption time.

Adsorption isotherm

The isotherm study was carried out by varying the initial concentration (100–400 mg/L) at 293 K and natural pH. Isotherm models, namely Langmuir model and Freundlich model, were used to describe the interaction between the solute and the adsorbent. The Langmuir and Freundlich isotherm parameters and their correlation coefficients (R^2) are shown in Table 3, while the plots for both isotherm models

Table 2 | Intraparticle diffusion parameters for the adsorption of MO onto cross-linked chitosan/bentonite composite

C_0/mg/L	K_{p1}/mg/(g min$^{0.5}$)	K_{p2}/mg/(g min$^{0.5}$)	K_{p3}/mg/(g min$^{0.5}$)	B_1/mg/g	B_2/mg/g	B_3/mg/g	R_1^2	R_2^2	R_3^2
100	9.48	1.21	0.11	98.56	140.4	159.1	0.9909	0.9455	0.9237
150	18.45	4.71	0.82	82.18	134.9	186.1	0.9886	0.9871	0.8958
200	15.81	3.66	0.53	102.0	160.3	183.7	0.9667	0.9321	0.8847
400	9.87	2.36	0.04	157.3	172.8	232.8	0.9547	0.9975	0.9186

Table 3 | Langmuir and Freundlich isotherm parameters of MO adsorption onto cross-linked chitosan/bentonite composite

Isotherms	Parameters	293 K	303 K	313 K	323 K
Langmuir isotherm	Q	224.8	230.9	211.4	215.0
	b	0.0936	0.1090	0.6123	0.1575
	R^2	0.9942	0.9970	0.9998	0.9991
	χ^2	0.1457	1.7689	0.5585	1.2679
Freundlich isotherm	K_f	143.6	144.8	139.1	150.0
	n	14.48	14.76	11.80	14.84
	R^2	0.9930	0.9293	0.9837	0.9665
	χ^2	1.696	6.221	3.077	2.534

are presented in Figure 6. According to the results, the Langmuir model seemed to describe adsorption better than the Freundlich model isotherm in respect to these correlation coefficients obtained for both models.

To identify a suitable isotherm model for the adsorption of MO onto CCS/BT composite, chi-square analysis was carried out. The equivalent mathematical statement is presented as follows (Subramanyam & Das 2009):

$$\text{Chi-square} = \chi^2 = \sum \frac{(q_e - q_{e,cal})^2}{q_e} \tag{7}$$

where $q_{e,cal}$ is equilibrium capacity obtained by calculating from the model (mg/g) and q_e is the experimental data of

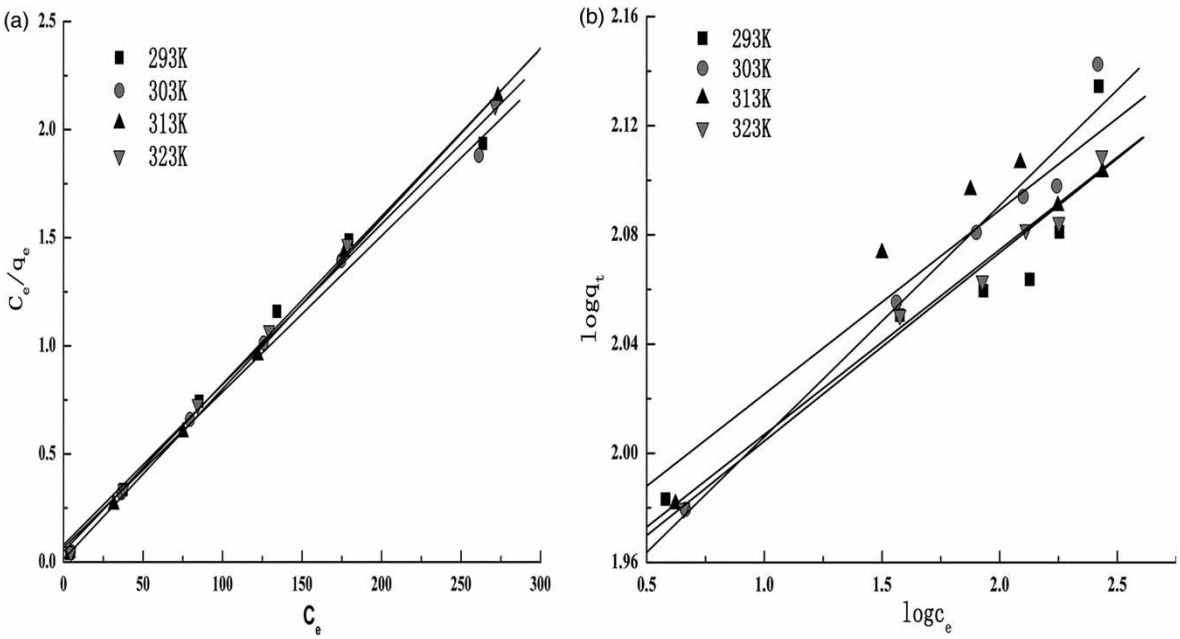

Figure 6 | Adsorption isotherm models of MO onto cross-linked chitosan/bentonite composite: Langmuir (a) and Freundlich (b).

the equilibrium capacity(mg/g). If data from the model are similar to the experimental data, χ^2 will be a small number, while if they differ, χ^2 will be a bigger value. The results of chi-squared analysis are presented in Table 3. The lower χ^2 values of the Langmuir isotherm than the Freundlich further confirmed the applicability of the Langmuir model for the sorption of MO on CCS/BT composite.

The Langmuir model predicts the formation of a monolayer of the adsorbate on the adsorbent surface (Vasconcelos *et al.* 2008). The maximum monolayer adsorption (Q_{max}) of MO obtained by CCS/BT composite was 224.8 mg/g. In the present study, the adsorption capacity of CCS/BT was compared to other adsorbents in terms of MO removal. From Table 4, CCS/BT has a higher adsorption capacity, suggesting that it was a promising adsorbent for the adsorption of MO from aqueous solutions.

CONCLUSIONS

The aim of this study was to prepare and characterize CCS/BT composite, and investigate its ability to be used for the adsorption of MO. The result from XRD analysis showed CCS intercalated in bentonite. The adsorption capacity of MO onto CCS/BT composite was much higher than that of cross-linked chitosan or bentonite. Also, the adsorption of MO onto CCS/BT composite was dependent on the ratio of chitosan to bentonite and contact time. The pH value had a minor impact on MO adsorption in a wide pH range. The adsorption kinetics obeyed the pseudo-second-order model, and the isotherm followed the Langmuir model. The adsorption capacity calculated by the Langmuir model was 224.8 mg/g. The cost of adsorbent was reduced by compositing bentonite with chitosan, and its adsorption capacity improved due to the intercalation of chitosan in bentonite. Therefore, CCS/BT composite might be a promising adsorbent for the removal of MO from aqueous solutions.

Table 4 | Comparison of the maximum monolayer adsorption capacities of MO onto various adsorbents

Adsorbent	Adsorption capacity (mg/g)	Reference
Mesoporous Y-Fe_2O_3/SiO_2 nanocomposites	476	Deligeer *et al.* (2011)
Activated carbon modified by silver nanoparticles	0.69	Pal *et al.* (2013)
Calcined Lapindo volcanic mud	333.3	Jalil *et al.* (2010)
Bentonite	33.8	Leodopoulos *et al.* (2012)
Maghemite/chitosan films	29	Jiang *et al.* (2012)
Chitosan/alumina composite	33	Zhang *et al.* (2011)
Chitosan	34.83	Saha *et al.* (2010)
Acid-modified carbon-coated monolith	147.1	Cheah *et al.* (2013)
Cross-linked chitosan/bentonite composite	224.8	This study

ACKNOWLEDGEMENT

The financial support extended to the projects by the National Natural Science Foundation of China (Grant No. 51003086) is gratefully acknowledged.

REFERENCES

Anirudhan, T. S. & Rijith, S. 2012 Synthesis and characterization of carboxyl terminated poly (methacrylic acid) grafted chitosan/bentonite composite and its application for the recovery of uranium (VI) from aqueous media. *J. Environ. Radioactiv.* **106**, 8–19.

Anirudhan, T. S., Rijith, S. & Tharun, A. R. 2010 Adsorptive removal of thorium(IV) from aqueous solutions using poly (methacrylic acid)-grafted chitosan/bentonite composite matrix: process design and equilibrium studies. *Colloid. Surface. A.* **368**, 13–22.

Bansiwal, A., Thakre, D., Labhshetwar, N., Meshram, S. & Rayalu, S. 2009 Fluoride removal using lanthanum incorporated chitosan beads. *Colloid. Surface. B.* **74**, 216–224.

Cao, J., Lin, J., Fang, F., Zhang, M. & Hu, Z. 2014 A new absorbent by modifying walnut shell for the removal of anionic dye: kinetic and thermodynamic studies. *Bioresource Technol.* **163**, 199–205.

Cheah, W., Hosseini, S., Ali Khan, M., Chuah, T. G. & Choong, T. S. Y. 2013 Acid modified carbon coated monolith for methyl orange adsorption. *Chem. Eng. J.* **215–216**, 747–754.

Chen, S., Zhang, J., Zhang, C., Yue, Q., Li, Y. & Li, C. 2010 Equilibrium and kinetic studies of methyl orange and methyl violet adsorption on activated carbon derived from *Phragmites australis*. *Desalination* **252**, 149–156.

Deligeer, W., Gao, Y. W. & Asuha, S. 2011 Adsorption of methyl orange on mesoporous Y-Fe_2O_3 /SiO_2 nanocomposites. *Appl. Surf. Sci.* **257**, 3524–3528.

Fan, H., Zhou, L., Jiang, X., Huang, Q. & Lang, W. 2014 Adsorption of Cu^{2+} and methylene blue on dodecyl sulfobetaine surfactant-modified montmorillonite. *Appl. Clay Sci.* **95**, 150–158.

Harmoud, H., Gaini, A., Daoudi, L. E., Rhazi, M., Boughaleb, Y., El Mhammedi, M. A., Migalska-Zalas, A. & Bakasse, M. 2014

Removal of 2,4-D from aqueous solutions by adsorption processes using two biopolymers: chitin and chitosan and their optical properties. *Opt. Mater.* **36**, 1471–1477.

Hena, S. 2010 Removal of chromium hexavalent ion from aqueous solutions using biopolymer chitosan coated with poly (3-methyl thiophene) polymer. *J. Hazard. Mater* **181**, 474–479.

Ho, Y. S. 2004 Citation review of Langergren kinetic rate equation on adsorption reactions. *Scientometrics* **59**, 171–177.

Jalil, A. A., Triwahyono, S., Ha Adam, S., Rahim, N. D., Aziz, M. A., Hairom, N. H. H., Razali, N. A. M., Abidin, M. A. Z. & Mohamadiah, M. K. A. 2010 Adsorption of methyl orange from aqueous solution onto calcined Lapindo volcanic mud. *J. Hazard. Mater* **181**, 755–762.

Jiang, R., Fu, Y. Q., Zhu, H. Y., Yao, J. & Xiao, L. 2012 Removal of methyl orange from aqueous solutions by magnetic maghemite/chitosan nanocomposite films: adsorption kinetics and equilibrium. *J. Appl. Polym. Sci.* **125**, E540–E549.

Kellner, R., Mermet, J. M. & Otto, M. 1998 *Analytical Chemistry*. Wiley, New York.

Leodopoulos, C., Doulia, D., Gimouhopoulos, K. & Triantis, T. M. 2012 Single and simultaneous adsorption of methyl orange and humic acid onto bentonite. *Appl. Clay Sci.* **70**, 84–90.

Li, J. Y., Sui, K., Liu, R., Zhao, X., Zhang, Y., Liang, H. & Xia, Y. 2012 Removal of methyl orange from aqueous solution by calcium alginate/multi-walled carbon nanotubes composite fibers. *Energy Procedia* **16**, 863–868.

Nair, V., Panigrahy, A. & Vinu, R. 2014 Development of novel chitosan-lignin composites for adsorption of dyes and metal ions from wastewater. *Chem. Eng. J.* **254**, 491–502.

Nesic, A. R., Velickovic, S. J. & Antonovic, D. G. 2012 Characterization of chitosan montmorillonite membranes as adsorbents for Bezactive Orange V-3R dye. *J. Hazard. Mater.* **209–210**, 256–263.

Nesic, A. R., Velickovic, S. J. & Antonovic, D. G. 2013 Modification of chitosan by zeolite A and adsorption of Bezactive Orange16 from aqueous solution. *Compos. Part B- Eng.* **53**, 145–151.

Nguyen, T. A. H., Ngo, H. H., Guo, W. S., Zhang, J., Liang, S., Yue, Q. Y., Li, Q. & Nguyen, T. V. 2013 Applicability of agricultural waste and by-products for adsorptive removal of heavy metals from wastewater. *Bioresource Technol.* **148**, 574–585.

Pal, J., De, M. K., Deshmukh, D. K. & Verm, D. 2013 Removal of methyl orange by activated carbon modified by silver nanoparticles. *Appl. Water Sci.* **3**, 367–374.

Pereira, F. A. R., Sousa, K. S., Cavalcanti, G. R. S., Fonseca, M. G., Antônio, G. S. & Alves, A. P. M. 2013 Chitosan-montmorillonite biocomposite as an adsorbent for copper (II) cations from aqueous solutions. *Int. J. Biol. Macromol.* **61**, 471–478.

Pitakpoolsil, W. & Hunsom, M. 2013 Adsorption of pollutants from biodiesel wastewater using chitosan flakes. *J. Taiwan Inst. Chem. Eng.* **44**, 963–971.

Repo, E., Warchoł, J. K., Bhatnagar, A., Mudhoo, A. & Sillanpää, M. 2013 Aminopolycarboxylic acid functionalized adsorbents for heavy metals removal from water. *Water Res.* **47**, 4812–4832.

Saha, T. K., Bhoumik, N. C., Karmaker, S., Ahmed, M. G., Ichikaw, H. & Fukumori, Y. 2010 Adsorption of methyl orange onto chitosan from aqueous solution. *J. Water Resour. Prot.* **2**, 898–906.

Saravanan, D., Gomathi, T. & Sudha, P. N. 2013 Sorption studies on heavy metal removal using chitin/bentonite biocomposite. *Int. J. Biol. Macromol.* **53**, 67–71.

Subramanyam, B. & Das, A. 2009 Linearized and non-linearized isotherm models comparative study on adsorption of aqueous phenol solution in soil. *Int. J. Environ. Sci. Technol.* **6**, 633–640.

Sun, X., Huang, W., Ma, Z., Lu, Y. & Shen, X. 2013 A novel approach for removing 2-naphthol from wastewater using immobilized organo-bentonite. *J. Hazard. Mater.* **252–253**, 192–197.

Tirtom, V. N., Dincer, A., Becerik, S., Aydemir, T. & Celik, A. 2012 Comparative adsorption of Ni(II) and Cd(II) ions on epichlorohydrin crosslinked chitosan clay composite beads in aqueous solution. *Chem. Eng. J.* **197**, 379–386.

Tripathy, S. S., Bersillon, J. L. & Gopal, K. 2006 Removal of fluoride from drinking water by adsorption onto alum-impregnated activated alumina. *Sep. Purif. Technol.* **50**, 310–317.

Vasconcelos, H. L., Camargo, T. P., Goncalves, N. S., Neves, A., Laranjeira, M. C. M. & Favere, V. T. 2008 Chitosan crosslinked with a metal complexing agent: synthesis, characterization and copper(II) ions adsorption. *React. Funct. Polym.* **68**, 572–579.

Wan Ngah, W. S., Teong, L. C. & Hanafiah, M. A. K. M. 2011 Adsorption of dyes and heavy metal ion by chitosan films: a review. *Carbohyd. Polym.* **83**, 1446–1456.

Wan Ngah, W. S., Teong, L. C., Toh, R. H. & Hanafiah, M. A. K. M. 2012 Utilization of chitosan-zeolite composite in the removal of Cu(II) from aqueous solution: adsorption, desorption and fixed bed column studies. *Chem. Eng. J.* **209**, 46–53.

Wan Ngah, W. S., Teong, L. C., Toh, R. H. & Hanafiah, M. A. K. M. 2013 Comparative study on adsorption and desorption of Cu(II) ions by three types of chitosan-zeolite composites. *Chem. Eng. J.* **223**, 231–238.

Weber, W. J. & Morris, J. C. 1964 Equilibria and capacities for adsorption on carbon. *J. Sanitary Eng. Div.* **90**, 79–107.

Wen, Y., Tang, Z., Chen, Y. & Gu, Y. 2011 Adsorption of Cr(VI) from aqueous solutions using chitosan-coated fly ash composite as biosorbent. *Chem. Eng. J.* **175**, 110–116.

Wu, F., Tseng, R. & Juang, R. 2001 Kinetic modeling of liquid-phase adsorption of reactive dyes and metal ions on chitosan. *Water Res.* **35**, 613–618.

Yao, Y., He, B., Xu, F. & Chen, X. 2011 Equilibrium and kinetic studies of methyl orange adsorption on multiwalled carbon nanotubes. *Chem. Eng. J.* **170**, 82–89.

Zha, S., Zhou, Y., Jin, X. & Chen, Z. 2013 The removal of amoxicillin from wastewater using organobentonite. *J. Environ. Manage.* **129**, 569–576.

Zhang, J., Zhou, Q. & Ou, L. 2011 Kinetic, isotherm, and thermodynamic studies of the adsorption of methyl orange from aqueous solution by chitosan/alumina composite. *J. Chem. Eng. Data* **57**, 412–419.

First received 7 May 2014; accepted in revised form 12 November 2014. Available online 24 November 2014